

# Novel Spatial Modulation Method Using Dual Scatterers for Wireless Power Transmission

# Akira Saitou<sup>1</sup>, Kohei Hasegawa<sup>1</sup>, Ryo Ishikawa<sup>1</sup>, Kazuhiko Honjo<sup>1</sup>

<sup>1</sup> Advanced Wireless Communication Research Center, the University of Electro-Communications  
1-5-1, Chofugaoka, Chofu, Tokyo, 182-8585, Japan, asaitou@uec.ac.jp

## 1. Introduction

Recent advances in the smart grid for electric power supply systems require long-distance wireless power transmission with smart wireless communication technology. Whereas power transmission and information transmission have been considered separately, a few papers have been proposed a method to transmit both power and information, in which wireless power transmission beam is modulated by signals [1]. However, since the peak average power ratios for the modulated beam are larger than unity, the communication was carried out only under the sacrifice of the power transmission efficiency. Thus, to utilize the maximum capacity of transmitted power, a novel wireless technology to transmit both power and information has been eagerly demanded.

To create signals from the un-modulated electromagnetic wave, a spatial modulation (SM) method has been proposed by the authors, where the signals are created by modulating transmission coefficient of the propagation channel [2]. This SM using an antenna and a single scatterer (SMSS) exploits the directivity control [3][4] for the communication scheme. By modulating scatterer's characteristics using a varactor, the array factor is modulated, which results in the modulated received electromagnetic wave. Whereas the modulation factor was not large enough, the method was verified to be effective both analytically and experimentally. However, there were a few problems to apply the method to the wireless power transmission applications. Firstly, whereas the radiation patterns of the antenna are remarkably directional in efficient power transmission systems, those of the scatterer are omni-directional. Thus, effective interference is realized only in the extremely limited direction. Secondly, since the modulation is realized by the interference between the waves caused by stimulated and induced currents, tight coupling between the antenna and the scatterer is necessary to improve the modulation factor, which tends to affect the main lobe and the efficiency of the power transmission.

In this paper, a novel SM method using dual scatterers (SMDS) are proposed, where the scatterers are located toward the sidelobe and in the far field region of the power transmitting antenna. In this case, affect on the power beam can be neglected. In addition, since the interference is realized by the waves scattered by the dual scatterers, effective interference can be realized in practical wider range directions, because both of the radiation patterns are omni-directional. Furthermore, since the affect on the power beam is solved, improvement of the modulation factor is examined by adopting a scatterer's structure embedded with lumped elements [5]. Whereas a varactor is assumed to be used to modulate the scatterer's characteristics, capacitors of varied sizes were used to relate each modulation state uniquely with the SMDS characteristics.

## 2. Analytical Expression for the SMDS

The configuration for this SMDS is shown in Fig. 1. Scatterers are located in the far-field region of the transmitting and receiving antennas. This performance can be expressed with the 4-port Z-matrix as follows, where two scatterers are short-terminated at the ports and  $R_0$  ( $50\Omega$ ) denotes the port impedance for the antennas:

$$\mathbf{0} = \mathbf{Z}_{11}\mathbf{I}_1 + \mathbf{Z}_{12}\mathbf{I}_2 + \mathbf{Z}_{13}\mathbf{I}_3 + \mathbf{Z}_{14}\mathbf{I}_4 \quad (1) \quad \mathbf{0} = \mathbf{Z}_{12}\mathbf{I}_1 + \mathbf{Z}_{22}\mathbf{I}_2 + \mathbf{Z}_{23}\mathbf{I}_3 + \mathbf{Z}_{24}\mathbf{I}_4 \quad (2)$$

$$\mathbf{V}_3 = \mathbf{Z}_{13}\mathbf{I}_1 + \mathbf{Z}_{23}\mathbf{I}_2 + \mathbf{R}_0\mathbf{I}_3 \approx -\mathbf{R}_0\mathbf{I}_3 \quad (3) \quad \mathbf{V}_4 = \mathbf{Z}_{14}\mathbf{I}_1 + \mathbf{Z}_{24}\mathbf{I}_2 + \mathbf{R}_0\mathbf{I}_4 \approx -\mathbf{R}_0\mathbf{I}_4 \quad (4)$$

The  $\mathbf{Z}_{34}$  was omitted because the receiving antenna is assumed to be located in the null direction of the transmitting antenna, which avoids the interference between the radiated and scattered carrier waves. Since the antennas are far from the scatterers, impedance-matching is almost maintained for

the antennas. The mutual impedances between the antennas and the scatterers can be approximated as follows, where  $\lambda$  denotes the wavelength in free space,  $r_{ij}$  denotes the distance between the antennas and the scatterers, and C is a constant:

$$Z_{ij} \approx C \frac{\lambda}{r_{ij}} e^{-jk r_{ij}} \quad i=1,2 \quad j=3,4 \quad (5)$$

With the Fraunhofer approximation [6], Eq. (6) was derived to express the current ratio  $A$  between those of the transmitting and receiving antennas, where  $\theta_0$  denotes the orientation of the scatterer set,  $\theta_1$  denotes the angle between the antennas,  $r_3$  and  $r_4$  denote the distances between the scatterer set and the antennas, and  $d$  denotes the distance between the scatterers.

$$A \equiv \frac{I_4}{I_3} \propto \frac{\lambda^2}{r_3 r_4} e^{-jk(r_3+r_4)} \frac{1}{2R_0} \times B \quad (6)$$

$$B = \frac{2(Z_{12}/Z_{11}Z_{22})\cos[kd \cos \theta_0 \sin(\theta_1/2)] - (1/Z_{11})\exp\{-jkd \sin \theta_0 \cos(\theta_1/2)\} - (1/Z_{22})\exp\{jkd \sin \theta_0 \cos(\theta_1/2)\}}{1 - Z_{21}^2/(Z_{11}Z_{22})} \quad (7)$$

Since the antennas are impedance-matched to  $50 \Omega$ , this current ratio is uniquely related with the received voltage or power. With (6) and (7), the modulated current for the receiving antenna ( $I_4$ ) can be obtained from the un-modulated current for the transmitting antenna ( $I_3$ ) by modulating the  $2 \times 2$  Z-matrix elements for the two scatterers.

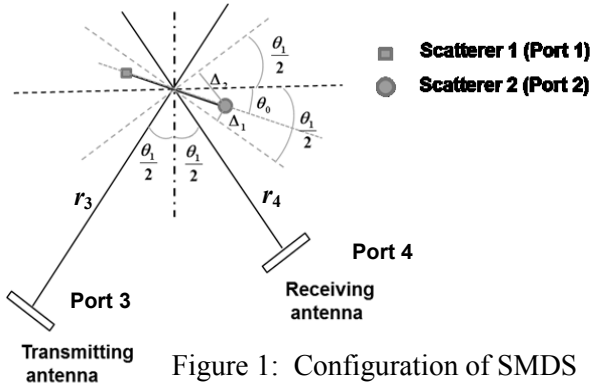


Figure 1: Configuration of SMDS

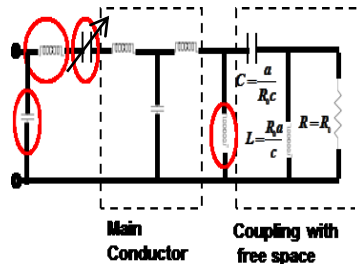
Since the amplitude modulation factor is given as follows [2], it approaches unity where the  $|A|_{\min}$  approaches null.

$$m_{AM} = \frac{|A|_{\max} - |A|_{\min}}{|A|_{\max} + |A|_{\min}} \quad (7)$$

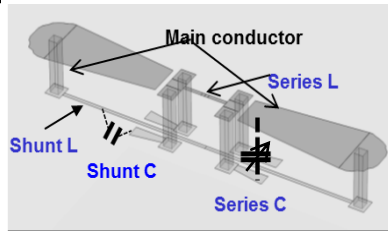
Thus the modulation factor can be improved where the current ratio becomes null in any state in the modulation. On the other hand,  $|A|_{\max}$  should be increased to increase the signal power. Thus, it is desirable that the scatterer set behaves as the director and the reflector of the Yagi-Uda arrays alternately according to the input signal.

### 3. Configurations and characteristics of the scatterer sets

For the Yagi-Uda arrays, the director and the reflector are interchanged by controlling the resonant frequency of the short-terminated element. Thus, to control the resonant frequency of the scattering element flexibly, an antenna structure embedded with lumped elements was used for the scatterers. The equivalent circuit and the configuration for the scatterer are shown in Fig. 2. Since the resonant frequency is effectively controlled by the series capacitor, the capacitor was selected to modulate the Z-parameters of the scatterer set. To imitate the modulation of the capacitance, the series capacitance was varied by changing the area of the parallel plate capacitor, as shown in Fig. 3. The length of the parallel plate was fixed for the scatterer 2, and the length was varied by  $\Delta$



(a) Equivalent circuit



(b) layout of the scatterer

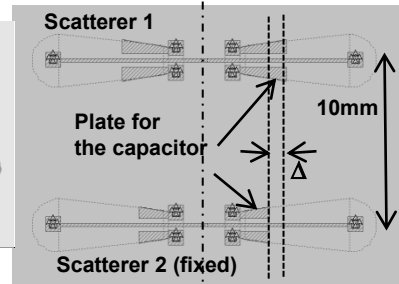
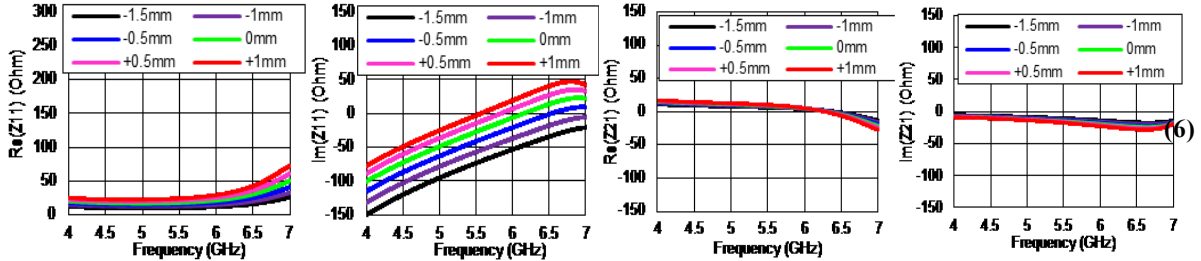


Figure 3: Pattern of a scatterer set  $\Delta=+1$  mm

Figure 2: Equivalent circuit and the pattern of the scatterer  
Circles denote the embedded lumped elements.

(-1.5mm, -1 mm, -0.5 mm, 0 mm, +0.5 mm, and +1 mm) for the scatterer 1. The patterns were laid out on a 1-mm thick FR-4 substrate ( $\epsilon_r = 4.6 \tan \delta = 0.01$ ). Z-parameters were simulated with an electro-magnetic simulator (SONNET<sup>TM</sup>) as shown in Fig. 4. The self-impedance of the scatterer 1 ( $Z_{11}$ ) varied with the length of the capacitor, and the resonant frequency was reduced with the increased capacitance. On the other hand, the mutual impedance was almost identical regardless of the varied scatterer 1. The self-impedance of the fixed scatterer 2 was almost identical. Thus, the current ratio  $A$  is considered to be modulated mainly by the variation of  $Z_{11}$ .

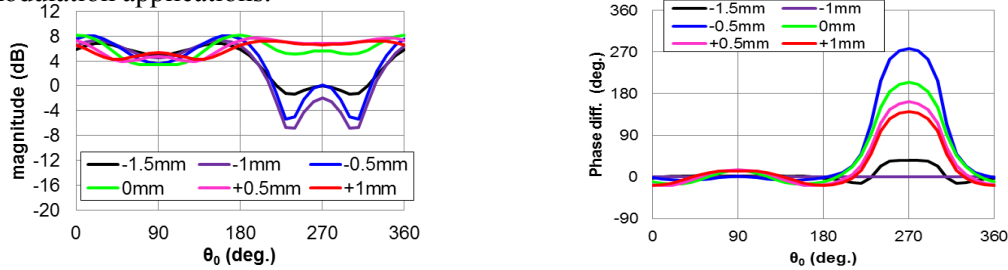


(a) Self-impedance ( $Z_{11}$ ) of the varied scatterer 1 (b) Mutual-impedance ( $Z_{21}$ )

Figure 4: Simulated Z-parameters for the scatterer sets.

#### 4. Simulated and measured characteristics of SMDS

With the simulated Z-parameters and (7), the current ratio  $B$  was estimated as shown in Fig. 5. At the 5.8 GHz power transmission band, the current ratio varied between -6.9 dB and 7.0 dB for the scatterer's orientation of  $\theta_0 = 270 \pm 40^\circ$ . This difference corresponds to the amplitude modulation index of 66 %, which is more than 10 times larger than that reported in [2]. Fig. 5(b) shows the phase variation of the current ratio  $B$ . This phase is expressed with the relative phase compared with the scatterer set of -1 mm capacitor length. The phase difference was maximum in the direction of  $\theta_0 = 270^\circ$ . The maximum difference was as large as  $270^\circ$ , which is also favorable for the phase modulation applications.

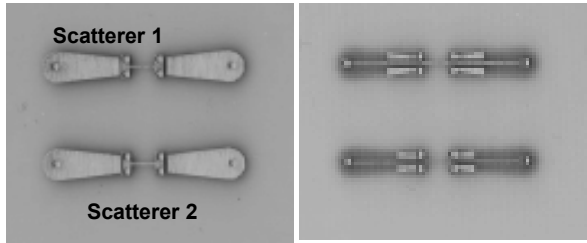


(a) Amplitude of the current ratio (b) Phase difference of the current ratio

Figure 5: Simulated characteristics of SMDS at 5.8 GHz ( $\theta_I=70^\circ$ )

The designed scatterer sets were fabricated as shown in Fig. 6. The substrate structure and the scatterer's patterns are the same with those shown in section 3. Fig. 7 shows a photograph of measurement. A horn antenna by mi-Wave (Model 261(159)-15) for the transmitting antenna and a dual ridge horn antenna by A.R.A (DRG118/A) for the receiving antenna were used. The scatterer sets were located 89 cm from the transmitting antenna, and 110 cm from the receiving antenna. The angle between the antennas ( $\theta_I$ ) was  $70^\circ$ . Where the scatterer set was removed, the transmission coefficient between the antennas was less than -70 dB. Fig. 8 shows the orientation ( $\theta_0$ ) effect on the received voltage ( $S_{21}$ ) at 5.8 GHz. The magnitude exhibited null in the direction of  $\theta_0 = 270 \pm 45^\circ$ , which agreed well with the simulated data. Measured magnitudes at  $225^\circ$  and  $315^\circ$  were slightly different, possibly because of the background without the scatterer set. The maximum magnitude difference for the scatterer sets was more than 15 dB, which corresponds to the modulation factor of 70 %. The phase was also varied by about  $280^\circ$  as shown in Fig. 8(b), which also agreed well with the simulated data. When the capacitance is modulated with a varactor, magnitude and phase of the

received voltage can be expected to be modulated to the extent. These values are considered to be sufficient for both the amplitude modulation and the phase modulation.



(a) front side (b) back side

Figure 6: Photograph of a fabricated scatterer set

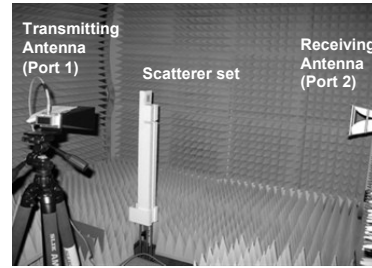
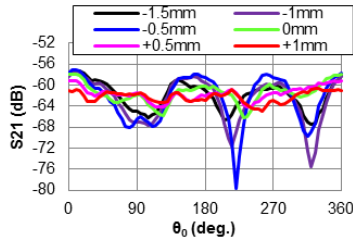
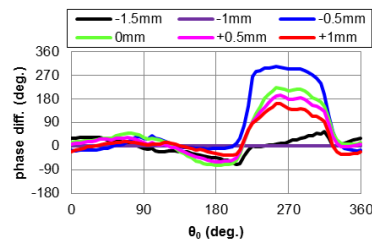


Figure 7: Photograph of measurement



(a) Amplitude of the received voltage



(b) Phase difference of the received voltage

Figure 8: Measured characteristics of SMDS at 5.8 GHz

## 5. Conclusion

A novel spatial modulation method appropriate for wireless power transmission applications was demonstrated using dual scatterers embedded with lumped elements. Analytical expression for the spatial modulation characteristics was derived, and the characteristics were verified with simulation and measurement by varying the embedded capacitor. The maximum measured difference of the received power was more than 15 dB and that of the phase was more than 270 degrees. The estimated amplitude modulation factor was more than 70 %.

## Acknowledgments

The authors wish to acknowledge the assistance and support by Guest Professor Yoichiro Takayama with the University of Electro-Communications. This work is partly funded by Ministry of Internal Affairs and Communications, Japan, for SCOPE Programme.

## References

- [1] S. Kawasaki, S. Kawai, T. Yamamoto, K. Takei, H. Seita, "A 5.8 GHz-band active integrated phased array antenna with wireless communication and power transmission functions for space and satellite use," 2008 China-Japan Joint Microwave Conf., p.p. 435-438, Sept. 2008
- [2] K. Hasegawa, Y. Hoshino, R. Ishikawa, A. Saitou and K. Honjo, "Spatial Modulation using Array Factor Control for Smart Grid Wireless Power Transmission," Proc. of the Asia-Pacific Microwave Conference, p.p. 837-840, Dec. 2011
- [3] R. Harrington, "Reactively Controlled Directive Arrays," *IEEE Trans. on Antennas and Propagation*, Vol. AP-26, No. 3, p.p. 390-395, May 1978
- [4] T. Ohira, Adaptive array antenna beamforming architectures as viewed by a microwave circuit designer," Proc. of the Asia-Pacific Microwave Conference, p.p. 828-833, Dec. 2000
- [5] Akira Saitou, Ryo Ishikawa, Yutaka Aoki, Kazuhiko Honjo, "Miniaturized dual-band differential-mode printed antennas embedded with broadband balun," Proc. of the Asia Pacific Microwave Conference, p.p. 1298-1301, Dec. 2011
- [6] Per-Simon Kildal, "Foundations of antennas," p.p. 42-44, Studentlitteratur, Lund, 2002